REDUCED MUTUAL COUPLING FOR THROUGH WALL RADARS USING ORTHOGONALLY POLARIZED ANTENNAS

by

Guntaas Kaur

Under the supervision of

Shobha Sundar Ram

Indraprastha Institute of Information Technology, Delhi

December 2017

REDUCED MUTUAL COUPLING FOR THROUGH WALL RADARS USING ORTHOGONALLY POLARIZED ANTENNAS

by

Guntaas Kaur

Submitted in partial fulfillment of the requirements for the degree of

Master of Technology

in

Electronics and Communication Engineering

to

Indraprastha Institute of Information Technology, Delhi

December 2017

Certificate

This is to certify that the thesis titled "**Reduced Mutual Coupling for Through Wall Radars using Orthogonally Polarized Antennas**" being submitted by **Guntaas Kaur** to the Indraprastha Institute of Information Technology Delhi, for the award of the Master of Technology, is an original research work carried out by her under my supervision. In my opinion, the thesis has reached the standards fulfilling the requirements of the regulations relating to the degree.

The results contained in this thesis have not been submitted in part or full to any other university or institute for the award of any degree/diploma.

December, 2017

Shobha Sundar Ram
Department of Electronics and Communication Engineering
Indraprastha Institute of Information Technology Delhi
New Delhi 110020

Abstract

There has been a growing interest in building through-the-wall radars (TWR) for law enforcement, security and biomedical applications for tracking humans in urban environments. Designing the antennas for such systems is a challenging task due to constraints such as mutual coupling effects between antenna elements, cross-polarization in dual-polarized operation and adverse wall effects on the elements' input impedance and gain when the array is operating in close proximity to an exterior wall.

The objective of this thesis is to provide a transmitter-receiver antenna configuration with low mutual coupling between the transmitter and receiver antenna elements, wide frequency bands of operation, high gain and wide field-of-view. The quadrifilar helix antennas were chosen because of their high gain, wide bandwidth and compact size. The mutual coupling between the transmitter and receiver was reduced by using oppositely polarized antennas. Multiple helical antennas were configured in a manner to obtain high field-of-view at both the transmitter and receiver.

The experiments for this thesis work have been performed over the range of 3-4GHz. The resonant frequency for the quadrifilar helix antenna is chosen to be 3.4GHz. The antennas have been simulated on Computer Simulation tool (CST), then fabricated and mounted. The design of the feeding network of the antenna has been done in the Advanced System Design (ADS) tool. Final measurements of mutual coupling in the system have been done with the help of a vector network analyzer (VNA). The system is tested in line-of-sight conditions with and without a target.

Acknowledgements

I express my sincere gratitude to my thesis supervisor Dr. Shobha Sundar Ram for her valuable guidance and inspiration throughout my thesis work. The unwavering faith shown by her in my abilities is extremely valuable for me. It was a great honor for me to work with her who has always appreciated my work and helped me overcome the difficulties I faced.

I would like to thank Mr. Rahul Gupta for helping me out with the fabrication work and providing me the required equipment in lab. I would also like to thank Mr. Abhijeet for helping me to create the mount of antenna in a short period of time.

I am grateful to the institute for providing such a wonderful work environment. I thank all my friends who stood by my side in the difficult times.

Finally, I wish to thank my brother and my parents for always having faith in me and helped me grow strong.

Guntaas Kaur

Contents

List of Figures

List of Tables

Chapter 1

Introduction

The attenuation of the radar signal through walls increases with the carrier frequency. However, low frequencies result in poor range, Doppler and direction-of-arrival resolutions. Researchers have found the frequency range of 1-4GHz to be the most optimal range for through wall applications. The design of antenna and all the experiments in this work has been done in the frequency range 3-4GHz.

While designing the antenna system for through-the-wall radar (TWR) applications, the characteristics of the system should be such that it is satisfactorily able to detect, image and distinguish moving and stationery targets and estimate their location, speed and dimension [1].

Few points are to be considered while designing the antenna

1. The antennas must be compact and of low profile to enable a portable radar system.
2. They should be configured to provide high direction-of-arrival resolution of the target as well as have a large field-of-view.
3. They should operate over a wide range of frequency since the down range resolution depends upon the operational bandwidth.
4. They should be sensitive to magnitude, phase and polarization of the scattered signal.
5. They should be easy to mount.
6. The receiving element should have high gain to minimize the signal distortion.

Large planar arrays are required for good azimuth - elevation resolution. However, they have the drawback of complexity and cost. This limitation can be partially overcome by using linear sub-arrays with synthetic aperture operation. One of the current designs for TWR is a fixed array with 4 transmit and 64 receive antenna elements used in bistatic or monostatic mode to image stationary targets as discussed in [1]. The system has two separable 1D arrays, one vertical and one horizontal. The vertical array has a linear subarray to depict details of the vertical building structure and the horizontal aperture comes into picture with the mechanical motion of linear subarray in horizontal direction. In this way the whole two-dimensional (2D) aperture is covered with a single linear array. The mutual coupling is reduced in horizontal direction as compared to a full 2D fixed array. This effect of reduction in mutual coupling can be very significant if antenna elements used are microstrip or printed type where the coupling is actually high in horizontal direction (radiating edge to radiating edge).

Printed microstrip type antenna elements are lightweight, compact and low profile with the disadvantage of narrow bandwidth. Few methods are described in [2, 3] to increase the bandwidth of antenna, making them quite attractive for TWRI applications. Examples are slotted patch antennas, stacked coupled patches giving a minimum bandwidth of 25% [4, 5], etc. Thus low profile linearly polarized TWRI receiving array can be designed with microstrip antennas with bandwidth enhancement techniques. However, they usually have low gain and high mutual coupling between the transmitter and receiver.

Horn antennas, printed spiral antennas, log periodic array antenna, biconical antenna, printed Vivaldi array, printed bowtie antenna are examples of ultra wideband antennas. Horn antennas and log periodic antennas have the disadvantage of bulky size. Thus, they are not very suitable for implementation in large TWRI receive arrays. One of these kinds of antenna that has been studied in [6] is the Circular E and Circular E complementary monopoles. They are planar antennas which offer UWB performance and are compact in size. Vivaldi antenna is found to be an excellent candidate for TWRI because of its simplicity, wide bandwidth, end-fire radiation pattern, low side lobes and high gain [7, 8]. However, it has a limited field of view.

Taking the above points into consideration, we propose to use the quadrifilar helix antennas for the TWR application in this thesis work. They have the advantage of wide bandwidth and a very compact size. Orthogonally polarized antennas have been designed for transmitter and receiver to avoid the mutual coupling. Multiple antennas with overlapping lobes have been configured to obtain a large field-of-view and direction-of-arrival estimation using amplitude monopulse technique. The antennas are mounted and the whole radar system is tested with target and without target in line-of-sight conditions.

The thesis is organized as follows. In the following chapter, we discuss the design principles of a helical antenna, followed by design principles of quadrifilar helix antenna in chapter 3. In chapter 2, we present the simulation studies of the effect of using orthogonally polarized transmitter and receiver antennas for a monostatic radar configuration. We present the measurement results in chapter 3 and conclude in chapter 4.

Chapter 2
Helical Antenna

Helical Antenna which comes under the category of broadband antennas is a conducting wire wound in the form of screw thread forming a helix [13]. Helical antenna with its geometrical configuration is shown in Figure 1. N is the number of turns, D is the diameter of helix and S is the spacing between each turn. L is the length of the antenna, L=NS. α is the pitch angle which is the angle formed by a line tangent to the helix wire and a plane perpendicular to the helix axis. C is the circumference of the helix.

$$\alpha = \tan^{-1}\left(\frac{S}{\pi D}\right) = \tan^{-1}\left(\frac{S}{C}\right)$$

The antenna operates in two principal modes, one is normal mode (broadside) and the other one is axial mode (end-fire) [13]. In the normal mode, the magnitude pattern has its maximum in a plane normal to the axis of helix, while in axial mode, the maximum is along the axis of the antenna. The axial mode is the most practical mode as it can easily achieve circular polarization over wide bandwidth and there is just one major lobe. The polarization of the antenna depends upon the winding sense of wire along the axis, whether right handed or left handed. The helix is small in size in case of normal mode. To excite in axial mode and to achieve the circular polarization, the circumference of the antenna should lie in the range $\frac{3}{4} < C/\lambda_o < \frac{4}{3}$ and the spacing should be about S $\cong \lambda_o/4$ where λ_o is the wavelength corresponding to resonant frequency. The pitch angle should be between $12° \leq \alpha \leq 14°$. The helix is usually used with a ground plane with size at least $3\lambda_o/4$. Coaxial feed is given to the helix from the bottom below the ground plane. The impedance of the terminal of helix is usually between 100 and 200 Ω. So, the impedance must be matched to the characteristic impedance of a coaxial feed which is usually 50Ω. One of the methods to match the impedance is to use an impedance matching rectangular or triangular strip of width w at the first ¼ turn of the helix wire [14, 15]. This strip is nearly touching the ground plane, covered with a dielectric slab of height, h

$$h = \frac{w}{\frac{377}{\sqrt{\epsilon_r} Z_o} - 2}$$

where, ϵ_r is the dielectric constant of slab

Z_o is the characteristic impedance of input transmission line

In this work, helical antenna has been designed in CST for the resonant frequency 3.4GHz. The following design parameters have been chosen

- Number of turns = 4
- Vertical Separation between turns =31.3mm
- Total Height, H=NS=125.2mm
- Diameter of turn, D=39.8mm
- Copper wire radius=0.25mm
- Diameter of Ground Plane > $\frac{3}{4}\lambda$ = 93.75mm
- Wavelength, λ = 88.23mm

A triangular copper strip is used for impedance matching at the beginning of the helix near the ground plane. The waveguide port is used to feed the antenna.

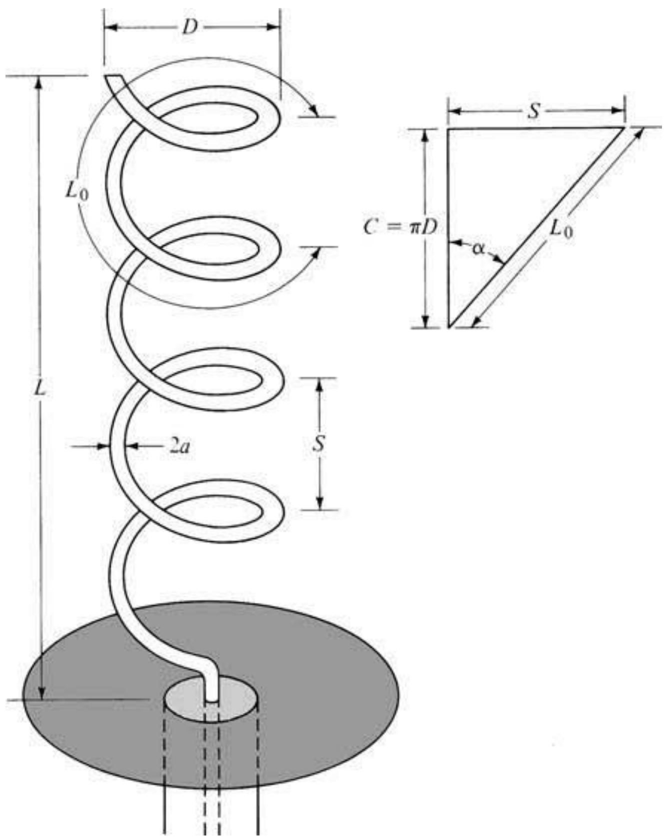

Figure 2.1: Helical Antenna with ground plane [13].

The simulated scattering parameter S_{11} is shown in Figure 2.2. The antenna is resonant at 3.4GHz and the -10dB bandwidth of the antenna is 15.3%.

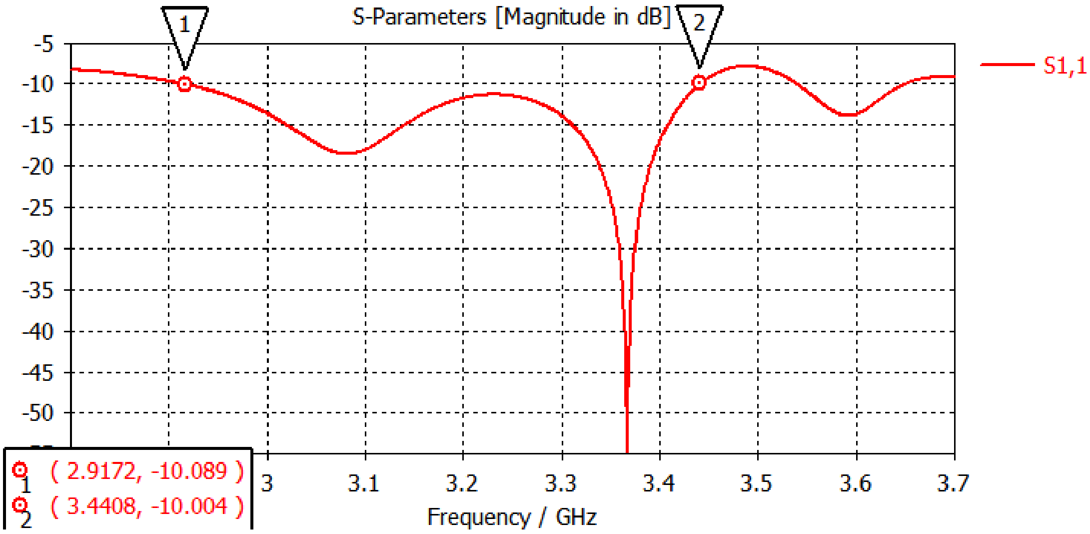

Figure 2.2: S_{11} plot for helical antenna in CST.

The gain of the antenna is highest at frequency 3.2GHz. The radiation pattern is shown in the polar plot in Figure 2.3. Gain is also noted for frequencies 3.3GHz and 3.4GHz. The values are 10.8dBi for 3.2GHz, 9.82dBi for 3.3GHz and 8.49dBi for 3.4GHz.

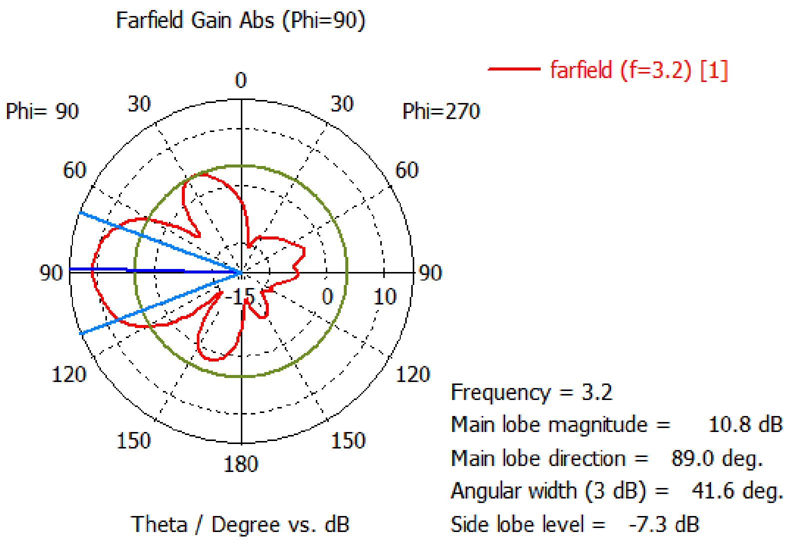

Figure 2.3: Gain plot at 3.2GHz.

The axial ratio plot for the antenna at 3.2GHz and 3.4GHz are shown in Figure 2.4 and 2.5 respectively.

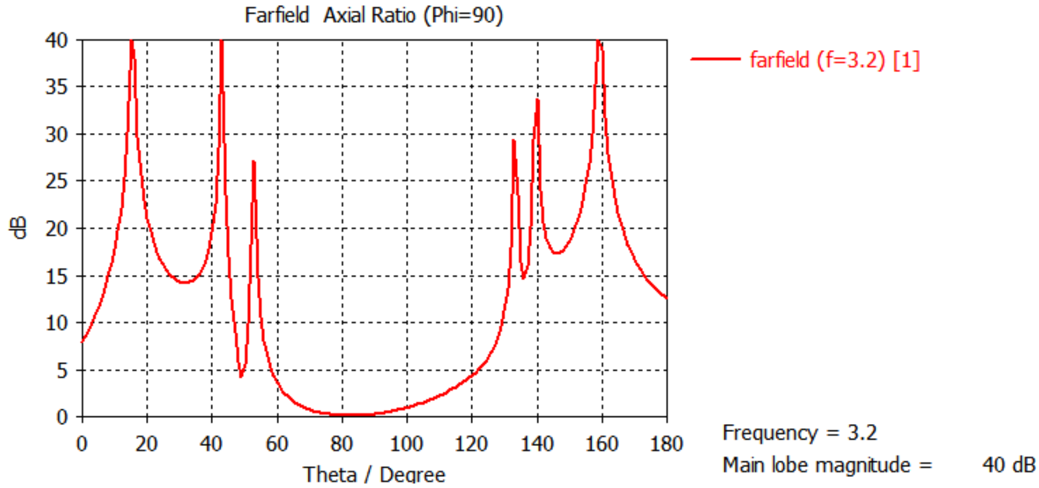

Figure 2.4: Axial Ratio plot for 3.2GHz

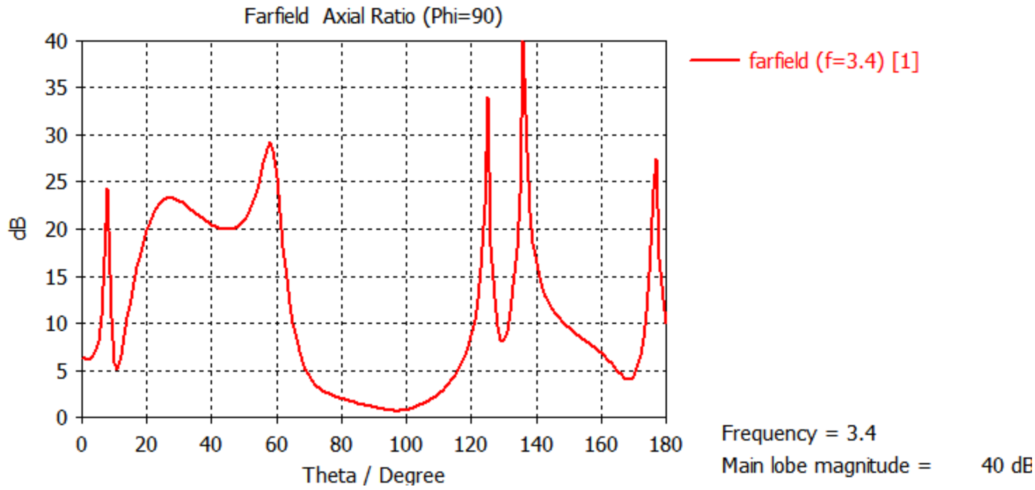

Figure 2.5: Axial Ratio plot for 3.4GHz

2.1. Mutual Coupling

Mutual coupling between two antennas is defined as the energy absorbed by one antenna acting as receiver when other antenna is operating nearby. In monostatic TWR systems, mutual coupling is an important issue. The scattered signal off the target at the radar receiver is usually much weaker than the direct signal from the co-located transmitter antenna. This is because of the two-way propagation loss of the radar signal through the wall medium. The mutual coupling among transmitter or receiver antenna elements is also a constraint when multiple antenna elements are present in receiver or transmitter such as in case of an array.

The design of array elements such that mutual coupling is reduced is discussed in [1]. The mutual coupling is greatly reduced in Synthetic aperture radar (SAR) where array elements are aligned in vertical direction and antenna is moved in horizontal direction. In this way there is no mutual coupling in horizontal direction [1].

We propose to tackle the problem of mutual coupling between receiver and co-located transmitter antenna by using two orthogonally polarized antennas. When the transmitter and receiver are of orthogonal circular polarizations, the direct coupling between them is reduced. However, the primary reflections off the target undergo sense reversal. As a result the signal from the target is picked up without polarization mismatch loss.

In our experimental study, we consider two helical antennas based on the previously described design parameters of opposite polarization. We simulate a two port network with the two antennas in CST and estimate their mutual coupling through the scattering parameter S_{21}. We consider 4 cases as shown below. In the first case, we consider two similarly polarized antennas (LHCP). They are placed side by side in a monostatic configuration in free space conditions. In the second case, a square metallic target plate is placed before the two antennas.

Case 1: Two Left hand circularly polarized antennas (LHCP-LHCP) are placed together shown in Figure 3.6.

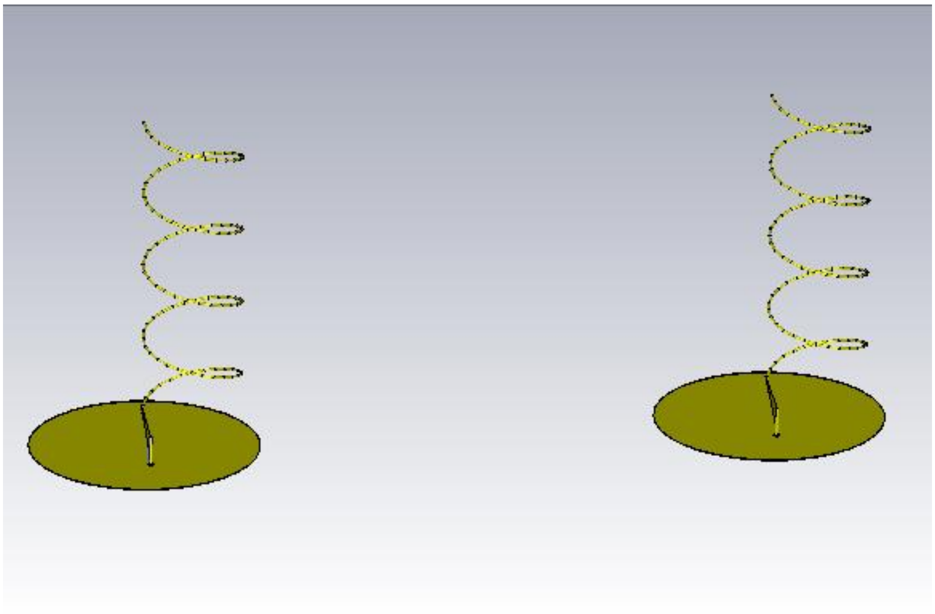

Figure 2.6: LHCP-LHCP configuration in CST.

Case 2: A copper plate of area 450 × 300 mm^2 is placed above LHCP- LHCP antennas as target as shown in Figure 2.7.

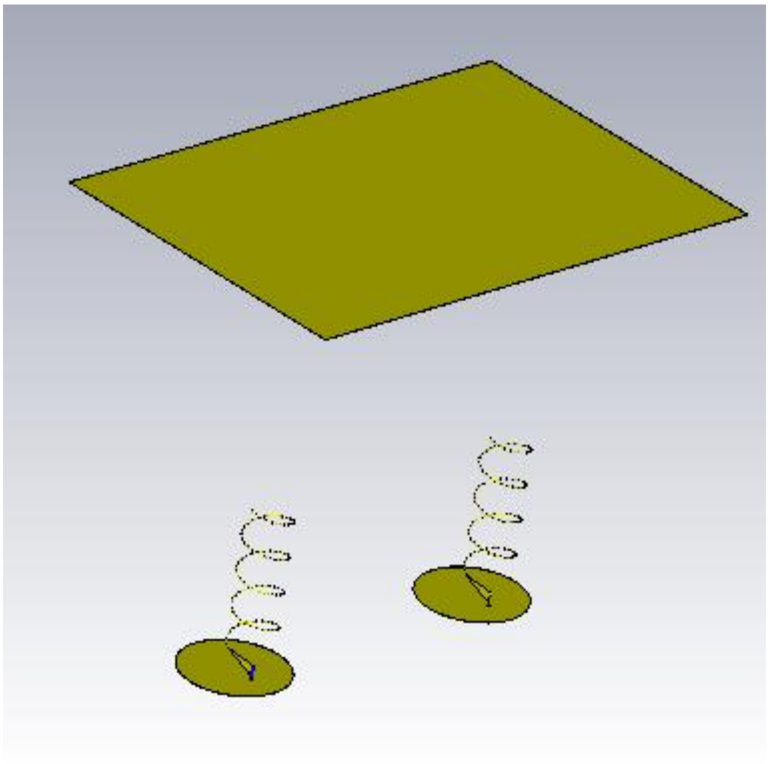

Figure 2.7: LHCP-LHCP configuration with plate.

Next, we consider two oppositely polarized antennas placed side by side as shown in Figure 2.8. In the final case, the square metallic plate is placed before the two antennas.

Case 3: LHCP-RHCP together as shown in Figure 2.8.

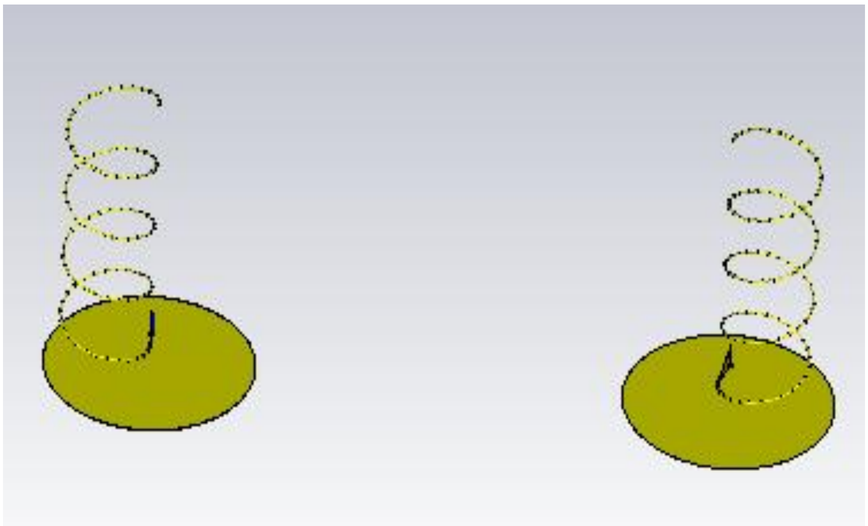

Figure 2.8: LHCP-RHCP configuration.

Case 4: LHCP-RHCP with copper plate.

The above cases are simulated in CST and S_{21} values in dB are noted for different frequencies as shown in Table no.2.1.

Table 2.1: S_{21} values at various frequencies.

Frequency (GHz)	**3.2**	**3.3**	**3.36**	**3.4**
LHCP-LHCP	-35.89	-44.72	-42.1	-39.6
LHCP-LHCP (with plate)	-31.07	-45.51	-47.02	-42.67
LHCP-RHCP	-36.13	-38.26	-38.89	-39.12
LHCP-RHCP (with plate)	-30.45	-30.08	-28.19	-27.46

Our hypothesis is that there should be higher S_{21} between antennas of same polarization as compared to antennas of opposite polarization. But when the target is introduced in the system with oppositely polarized antennas, only the signal reflected back from the target is received due to change of polarization after reflection The four cases are compared and the conclusions drawn out of the results are stated in Table 2.2.

Table 2.2: Observation table

Design Compared	**Hypothesis**	**Observations**

LHCP-LHCP & LHCP-LHCP with plate	S_{21} for case 2 should be less than case 1	• True for frequencies 3.3, 3.36 and 3.4 GHz. • False for 3.2GHz.
LHCP-LHCP & LHCP-RHCP	S_{21} for case 1 should be greater than case 3	• True for 3.2GHz. • False for 3.3 and 3.36GHz. • Values approximately same for 3.4GHz
LHCP-RHCP & LHCP-RHCP with plate	S_{21} for with plate design should be greater due to change of polarization due to reflection from plate	• True for all frequencies
LHCP-LHCP with plate & LHCP-RHCP with plate	S_{21} for LHCP-RHCP with plate should be greater as polarization becomes same after reflection	• True for all frequencies

Chapter 3

Quadrifilar Helix Antenna

3.1. Design

The drawback of the helical antenna, discussed in the previous chapter, is its large size which makes it unsuitable for portable radar applications. The quadrifilar helix antenna (QHA) is a compact alternative that provides circular polarization with very low sidelobe levels. QHA are widely used in global positioning systems (GPS) [12]. They also find applications in small mobile handheld devices, weather communication satellites, GNSS and many more. This antenna has 4 parallel helical windings. The extra windings tighten up the radiation pattern and reduce the sidelobe level. Each winding is excited with 90° phase progression either in clockwise or counter clockwise sense. The clockwise phase progression induces the “forward mode helix” i.e. when the wave appears to propagate from the feed point to open end along the helix. The radiation is endfire in this case. Similarly, the counter clockwise progression induces “backward mode helix” i.e. the wave appears to move towards the feed point. The radiation is backfire in this case. Regardless of the phase progression sense, the polarization of the antenna depends upon the sense of the helix winding, either right handed or left handed. The presence of the ground plane reverses the polarization of antenna due to reflection from the ground plane.

The antenna produces a cardioid shaped radiation pattern. The antenna can be short circuited or open circuited at the end as shown in Figure 3.1 [16].

A better version of QHA is the printed quadrifilar helix antenna (PQHA). In PQHA, the arms of the antenna are printed on the dielectric and then folded in the shape of a cylinder. They show better performance in terms of bandwidth, circular polarization and low cost. In the paper [12], a novel design of PQHA for improving the bandwidth is shown. They obtain a bandwidth of about 30%. In this work, both printed and wire QHA have been designed and fabricated. The

PQHA is used in the transmitter due to its large field-of-view and normal wire QHA is used as a receiver for the radar.

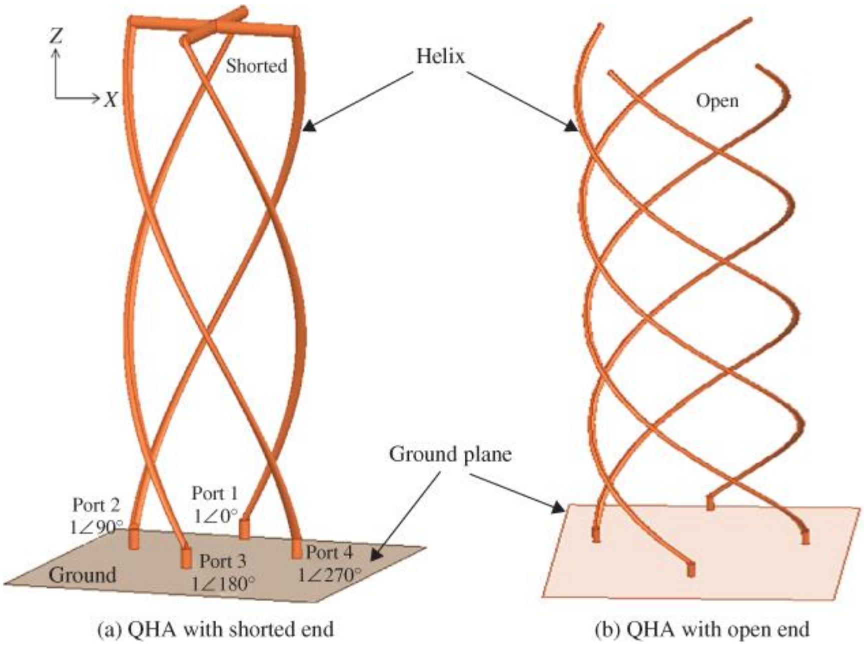

Figure 3.1: QHA with shorted and open end [16].

In this thesis, we design a QHA for the resonant frequency of 3.4GHz with the following design parameters.

- Height of QHA= 50mm
- Radius of QHA= 6mm
- Ground plane radius= 15mm
- Number of turns=1

The antenna height is reduced to less than half of that of the helical antenna resonating at the same frequency. Each helix arm is fed with waveguide port which is excited simultaneously in CST with the phase difference of 90°.

The S_{11} plot for QHA designed in CST is shown in Figure 3.2. The antenna is radiating close to 3.4GHz and the bandwidth is approximately 200 MHz.

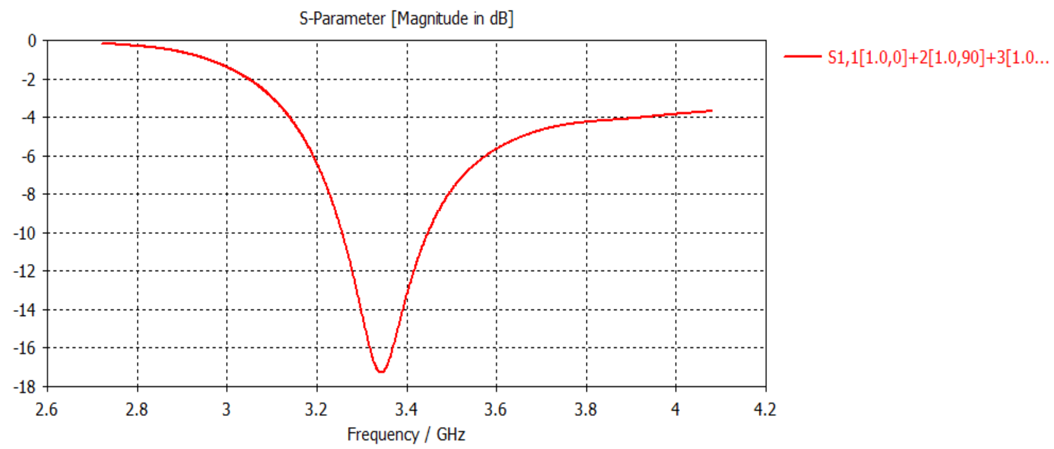

Figure 3.2: S_{11} plot for QHA.

The gain of the antenna at 3.4GHz comes out to be 4.49dBi as shown in Figure 3.3.

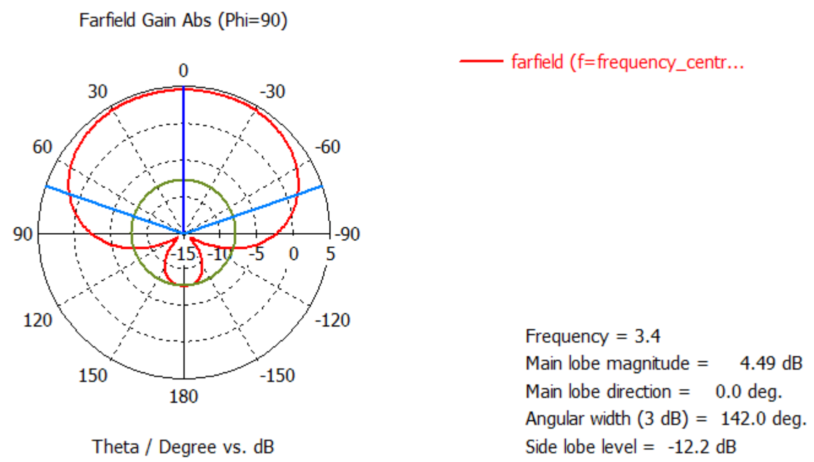

Figure 3.3: Gain plot at 3.4GHz

The axial ratio plot is shown for 3.4GHz in Figure 3.4. As can be seen from the plot, QHA has better performance as compared to helical antenna in terms of circular polarization. It gives a low value of axial ratio over wide angles.

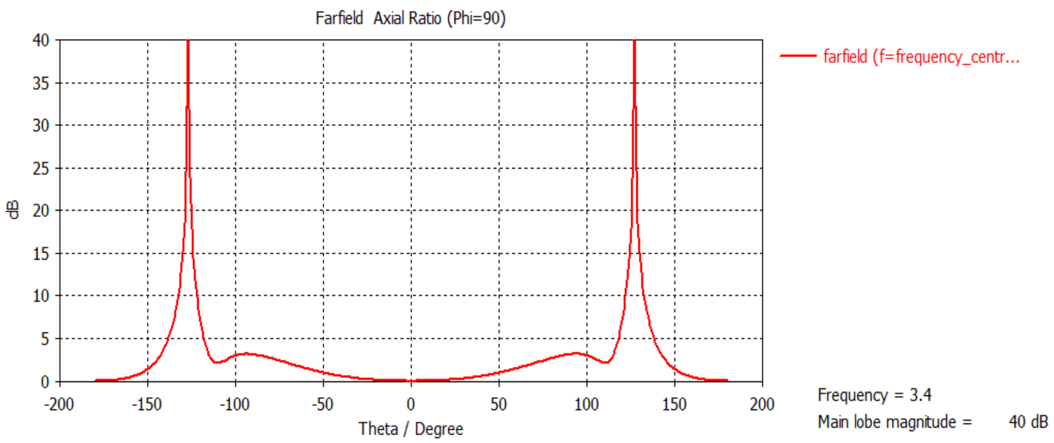

Figure 3.4: Axial Ratio plot at 3.4GHz

3.2. Feeding Network for the Quadrifilar Antenna

The QHA requires a quadrature feeding network designed to provide constant magnitude and progressive 90° phase shift to each helical winding. One option is to have a BALUNs based feeding system [9]. Alternately, this can also be achieved by using hybrids and couplers. A compact aperture coupled planar feeding network for broadband printed quadrifilar helix antenna is discussed in [10]. They have used hybrids to give phase difference and dual layers of substrate to make it more compact. Another method is to connect the input to a 180° hybrid, whose output is fed to two 90° hybrid [11].

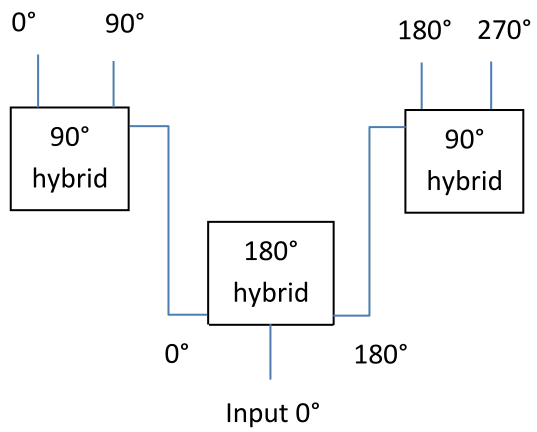

Figure 3.5: Feeding network for QHA.

This concept has been used while designing the feeding circuit in this work. A novel design of feeding network has been proposed in this work. A rat race coupler has been used to design 180° hybrid. Then Wilkinson power divider has been designed to give the final 90° phase shift. Thus, the four feeds collectively receive 0°, 90°, 180° and 270° excite signals. The feeding circuit is designed in the Advanced Design System (ADS) tool at 3.4GHz upon FR4 as substrate. The design is shown in Figure 3.6.

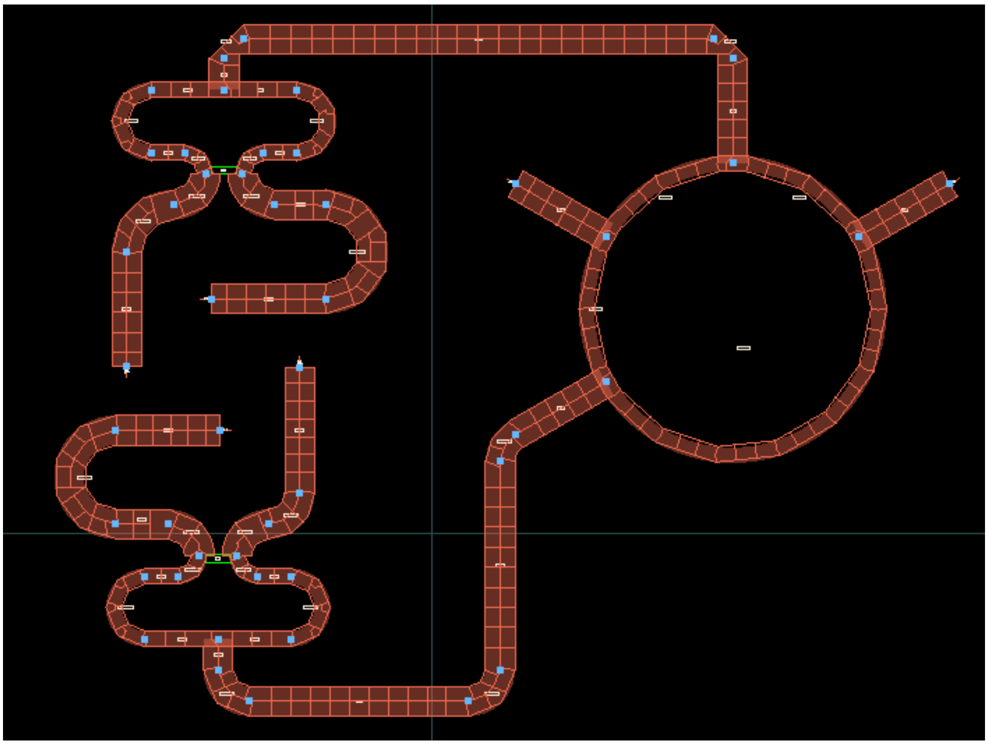

Figure 3.6: Feeding network layout in ADS.

Electromagnetic simulation is performed for the final design. The final phase plots for the 4 outputs with respect to the input signal at port 1 are shown in Figure 3.7. The output values are nearly equal to 0°, 90°, 180° and 270° (or -90°) for ports 2, 3, 4 and 5 respectively as shown in the figure. The design is compact and outputs are arranged in such a way that QHA can be easily placed upon it.

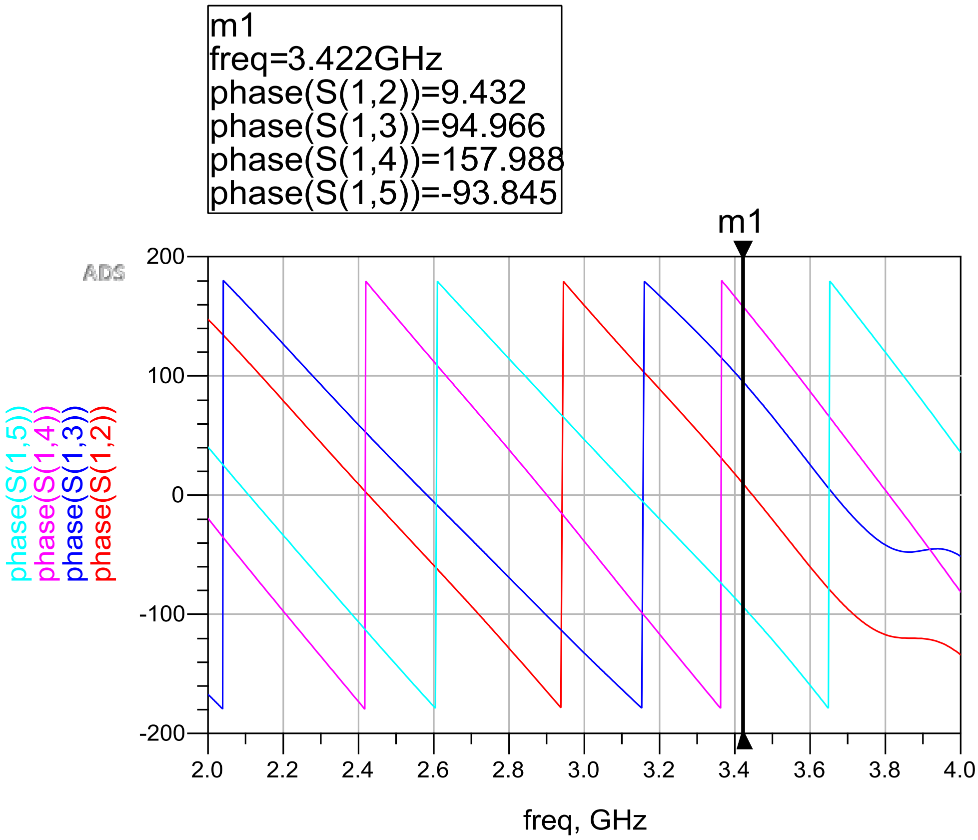

Figure 3.7: Phase plots for output ports in ADS.

3.3. Fabrication

The PQHA is built using the copper strips pasted upon a paper which is folded in the form of a cylinder. The antenna is placed upon the feeding circuit fabricated on PCB as shown in Figure 3.8. The measured S_{11} plots in VNA for both LHCP and RHCP antenna are shown in Figure 3.9 and 3.10 respectively. Results show that both the antennas radiate at 3.4GHz. The antenna gives a broad bandwidth of 17.6%. The PQHA is used as transmitter in the final radar system.

Figure 3.8: Fabricated PQHA.

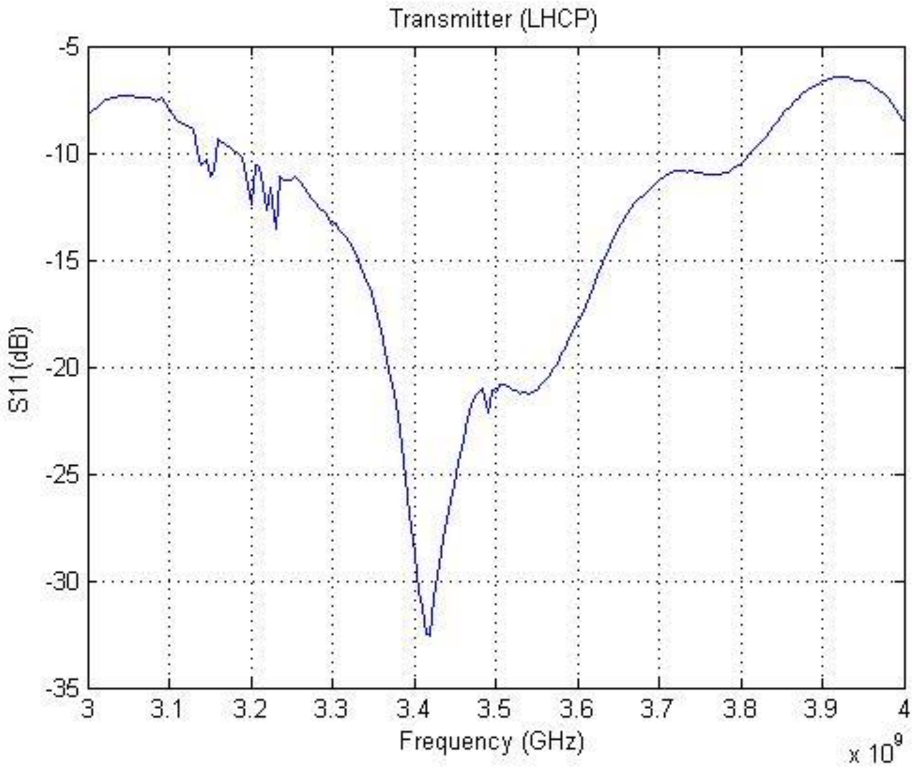

Figure 3.9: Measured S_{11} for transmitter PQHA (LHCP).

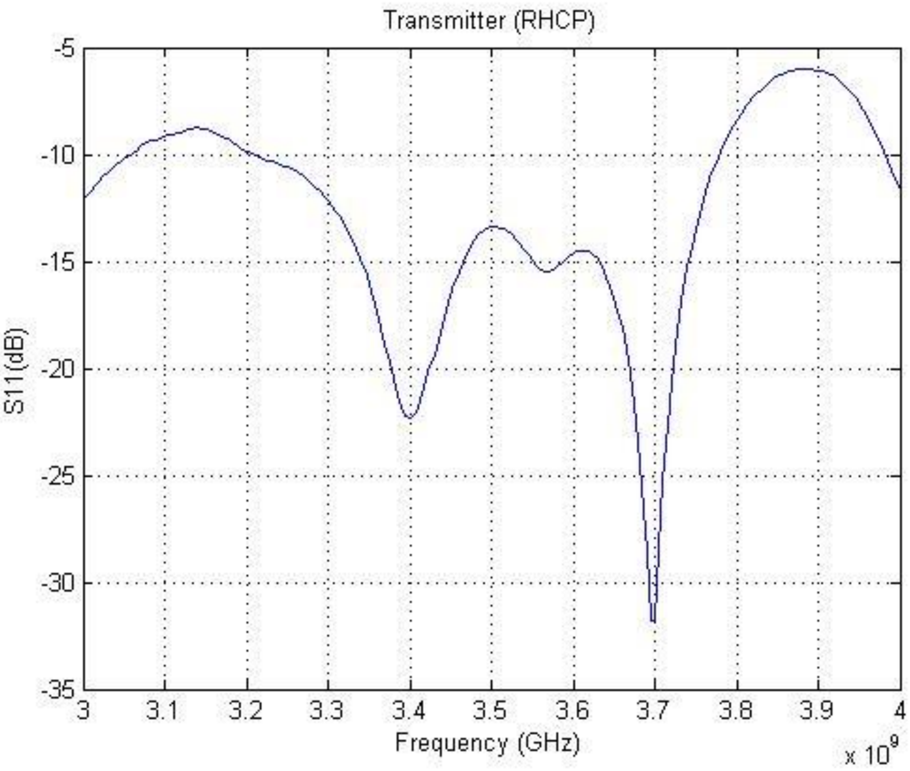

Figure 3.10: Measured S_{11} for transmitter PQHA (RHCP).

The final system consists of three receiver antennas built with wire QHA. Instead of copper strips, copper wire is used to design the antenna as shown in Figure 3.11.

Figure 3.11: Fabricated wire QHA

The S_{11} plots measured in VNA for three different receivers of same polarization are shown in Figures 3.12, 3.13 and 3.14. All the receiver antennas radiate at approximately 3.4GHz having wide bandwidth.

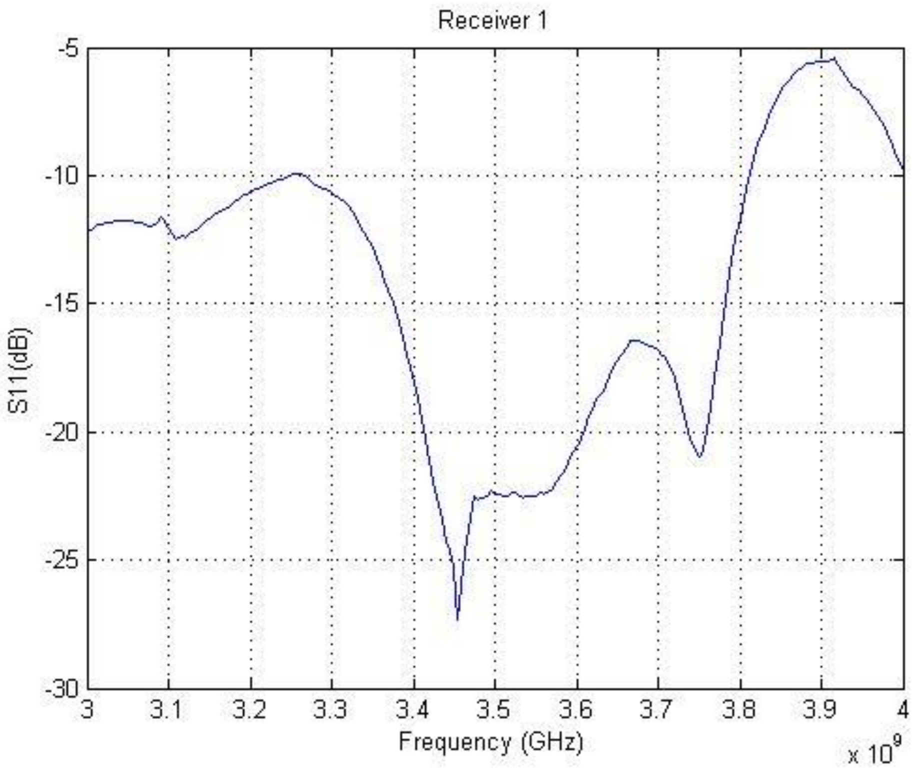

Figure 3.12: Measured S_{11} for Receiver 1.

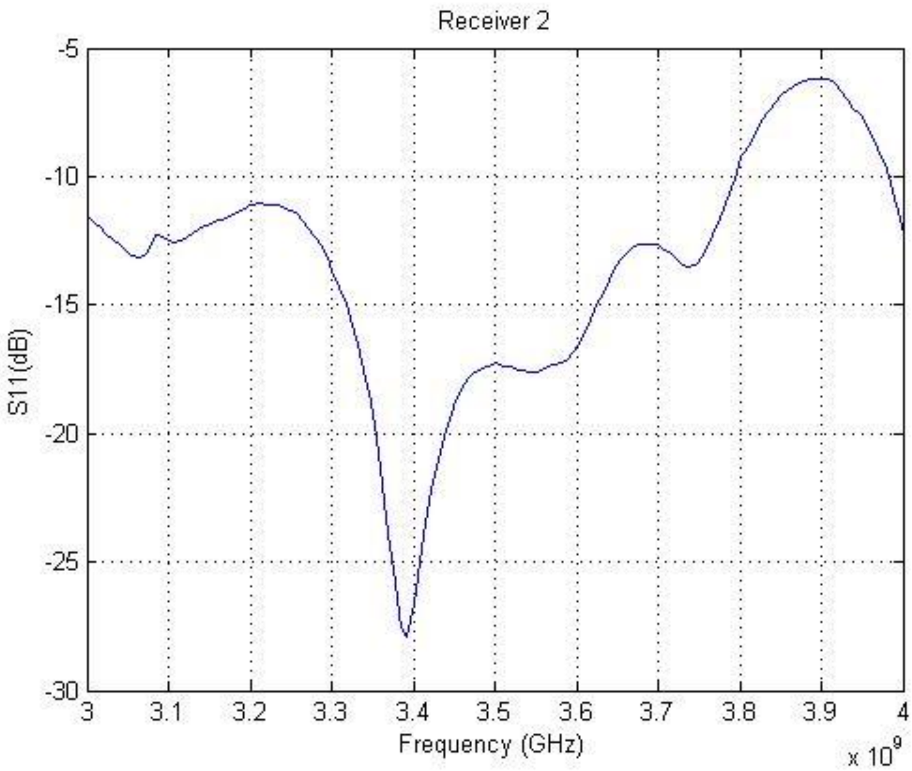

Figure 3.13: Measured S_{11} for Receiver 2.

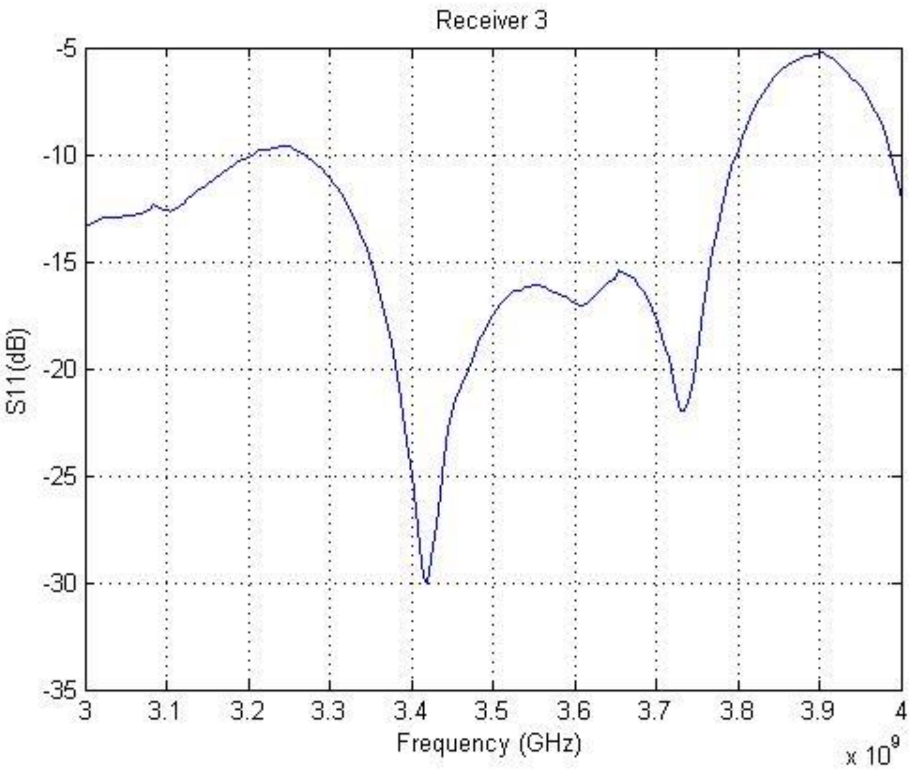

Figure 3.14: Measured S_{11} for Receiver 3.

3.4 Experimental Setup

In the final setup of radar, the transmitter consists of one PQHA and receiver consists of three wire QHA's which are 60° apart as shown in Figure 3.15.

Figure 3.15: Receiver setup with three antenna elements.

This setup simultaneously facilitates a wide field-of-view of the radar receiver and high gain. The direction-of-arrival of a target along the azimuth can be estimated using amplitude monopulse technique. Both the transmitter and receiver are mounted over a stand. All The three wire QHA in the receiver are of same polarization LHCP while the transmitter PQHA is designed in both LHCP and RHCP sense for the measurements. We consider square metal plate as the target as shown in Figure 3.16. The S_{21} measurements are made using a two port vector network analyzer (VNA). Port 1 of the VNA is connected to the transmitter PQHA while port 2 of the VNA is connected, in turn, to each of the three receiver antennas.

We again consider four cases as discussed in the previous chapter. In the first case, the transmitter antenna and the receiver antennas are of the same polarization. In the second case, we consider oppositely polarized transmitter and receiver QHA in the absence of a target. The results are presented in Table. 3.1. Next, we consider the cases where we have a target before the oppositely polarized antennas. These results are presented in Table 3.2.

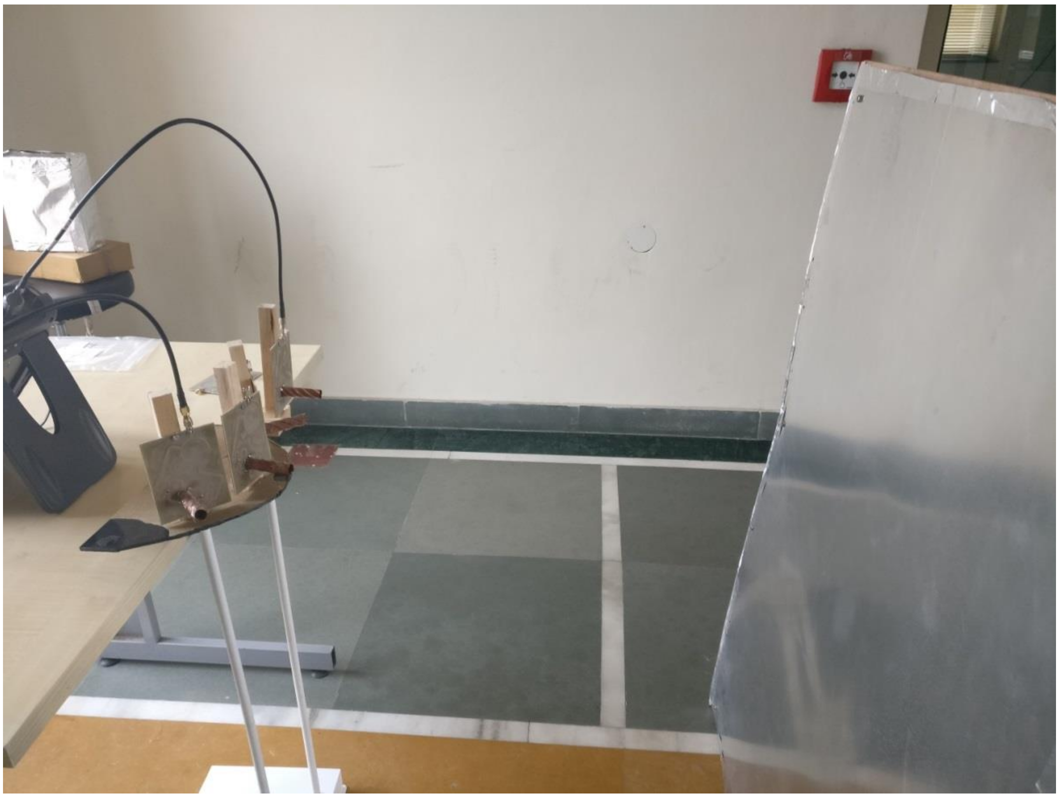

Figure 3.16: Experimental setup showing target (metal plate) in front of radar.

Table 3.1: S_{21} values at 3.4GHz without the target.

S21 (3.4GHz)	**Rx1 (LHCP)**	**Rx2 (LHCP)**	**Rx3 (LHCP)**
Tx (RHCP)	-38.86	-62.78	-62.97
Tx (LHCP)	-36.87	-55.95	-60.38

Table 3.2: S_{21} values at 3.4GHz with the target.

S21 (3.4GHz)	**Rx1 (LHCP)**	**Rx2 (LHCP)**	**Rx3 (LHCP)**
Tx (RHCP)	-36.35	-51.52	-54.77
Tx (LHCP)	-38.92	-67.62	-70.45

The four cases are compared and the conclusions drawn are listed in the Table. 3.3.

Table 3.3: Observation table.

Design Compared	Hypothesis	Observations
LHCP-LHCP & LHCP-LHCP with target	S21 for "with target case" should be less than "without target case" due to reflection from plate there would be change of Polarization.	• True for 3.4GHz
LHCP-LHCP & LHCP-RHCP	S21 for LHCP-LHCP should be greater than LHCP-RHCP due to same polarization.	• True for 3.4GHz
LHCP-RHCP & LHCP-RHCP with target	S21 for "with target case" should be greater than "without target case" due to change of polarization due to reflection from plate.	• True for 3.4GHz
LHCP-LHCP with target & LHCP-RHCP with target	S21 for LHCP-RHCP with target should be greater as polarization becomes same after reflection.	• True for 3.4GHz

The contrast is greatest for the second and third receivers as opposed to the first receiver where the proximity effects dominate.

Chapter 4

Conclusion

From the simulation and measurement results, we demonstrate that when oppositely polarized circular polarization antennas are used as transmitter and receiver antennas, the mutual coupling between the antennas is reduced. At the same time, the direct signal scattered from the target is enhanced. We also show that the QHA is a good candidate for TWR applications as it meets the desired specifications of wide bandwidth and compact size. Multiple QHA are configured to provide a wide field of view.

References

[1]. Amin, Moeness G., ed. *Through-the-wall radar imaging*. CRC press, 2016.

[2]. Kumar G. and K. P. Ray, *Broadband Microstrip Antennas*, Norwood, MA: Artech House, 2003.

[3]. Wong K. L., *Compact and Broadband Microstrip Antennas*, New York: Wiley, 2002.

[4]. Beigi, P., et al. "Bandwidth Enhancement of Small Square Monopole Antenna with Dual Band Notch Characteristics Using U-Shaped Slot and Butterfly Shape Parasitic Element on Backplane for UWB Applications." *Applied Computational Electromagnetics Society Journal* 30.1 (2015).

[5]. Weigand S., G. H. Huff, K. H. Pan, and J. T. Bernhard, Analysis and design of broad-band single-layer rectangular U-slot microstrip patch antennas, *IEEE Transactions on Antennas and Propagation*, 51, 457–468, March 2003.

[6]. Abbosh A. and M. Bialkowski, Design of ultra-wideband planar monopole antennas of circular and elliptical shape, *IEEE Transactions on Antennas and Propagation*, 56(1), 17–23, 2008.

[7]. Yang, Yunqiang, Y. Wang, and Aly E. Fathy. "Design of compact Vivaldi antenna arrays for UWB see through wall applications." *Progress In Electromagnetics Research* 82 (2008): 401-418.

[8]. Yang, Yunqiang, et al. "Development of an ultra wideband Vivaldi antenna array." *Antennas and Propagation Society International Symposium, 2005 IEEE*. Vol. 1. IEEE, 2005.

[9]. Ow, Steven G., and Peter J. Connolly. "Quadrifilar helix antenna." U.S. Patent No. 5,349,365. 20 Sep. 1994.

[10]. Caillet, Mathieu, et al. "A broadband folded printed quadrifilar helical antenna employing a novel compact planar feeding circuit." *IEEE Transactions on Antennas and Propagation* 58.7 (2010): 2203-2209.

[11]. Lamensdorf, David, Michael Smolinski, and Eddie Rosario. "Dual-band quadrifilar helix antenna." U.S. Patent No. 6,653,987. 25 Nov. 2003.

[12]. Letestu, Yoann, and Ala Sharaiha. "Broadband folded printed quadrifilar helical antenna." *IEEE Transactions on Antennas and Propagation* 54.5 (2006): 1600-1604.

[13]. Balanis C. A., *Antenna Theory, Analysis and Design*, 3rd edn, Hoboken, NJ: Wiley, 2005.

[14]. J. D. Kraus, *Antennas*, McGraw-Hill, New York, 1988.

[15]. J. D. Kraus, “A 50-Ohm Input Impedance for Helical Beam Antennas,” *IEEE Trans. Antennas Propagat.*, Vol. AP-25, No. 6, p. 913, November 1977.

[16]. Luo, Qi, and Fuguo Zhu. *Circularly polarized antennas*. John Wiley & Sons, 2013.